Monitoring the biomechanical response of individual cells under compression: a new compression device

E. A. G. Peeters C. V. C. Bouten C. W. J. Oomens F. P. T. Baaijens

Department of Biomedical Engineering, Eindhoven University of Technology, Eindhoven, The Netherlands

Abstract—*Skeletal muscle cells are sensitive to sustained compression, which can lead to the development of pressure sores. Although it is known that this type of tissue breakdown depends on the magnitude and duration of the applied load, the exact relationship between cell deformation and damage remains unclear. To gain more insight into this process, a method has been developed, that incorporates the use of a new loading device and confocal microscopy. The loading device is able to compress individual cells, either statically or dynamically, while measuring the resulting forces. Experiments can be performed under ideal environmental conditions, comparable with those of a CO_2 incubator. First compression experiments on C_2C_{12} mouse myoblasts showed the shape changes that cells undergo during static compression by the loading device. Calculations using the three-dimensional confocal images showed no change in volume and an increase in the surface area of the cell as a result of compression. The device presented here provides a useful way to monitor the biomechanical response of skeletal muscle cells during long-term compression experiments. Therefore it will contribute to the knowledge about strain-induced cell damage, as seen in pressure sores and other mechanically induced clinical conditions.*

Keywords—*Cell mechanics, Loading device, Compression, Confocal microscopy, Skeletal muscle, Pressure sores*

Med. Biol. Eng. Comput., 2003, **41**, 498–503

1 Introduction

STUDIES INVESTIGATING soft-tissue damage in animals have shown that skeletal muscle tissue is highly susceptible to sustained compression (NOLA and VISTNES, 1980; CAPLAN *et al.*, 1988). Depending on its magnitude and duration, the applied load causes tissue breakdown in the form of pressure sores (BARBENEL, 1991). This breakdown starts at the cellular level and is characterised by damage to the cell membrane and nucleus, followed by inflammatory reactions (BOUTEN *et al.*, 1999).

Previous studies have mainly focused on the biochemical environment of the cells (DANIEL *et al.*, 1982; KROUSKOP, 1983). These studies state that occlusion of lymph and blood vessels within the tissue impairs transport of nutrients and waste products from and to the cell. Although these factors contribute to cell damage, BOUTEN *et al.* (2001) showed that sustained cell deformation plays a significant role in the breakdown of muscle tissue, regardless of the nutrient and oxygen supply. However, the mechanisms whereby cell compression causes cell damage remain unclear. To understand this process better, a method needed to be developed to compress individual muscle cells and monitor their biomechanical response.

The biomechanical response can be subdivided into structural, mechanical and biochemical changes (DAVIES and TRIPATHI, 1993). For example, mechanical forces can induce cytoskeletal remodelling, thereby changing the internal structure and organisation of the cell (ELSON, 1988; GALBRAITH *et al.*, 1998). On the other hand, the structure and organisation of the cell and its environment influence the mechanical properties of the cell (CHEN and INGBER, 1999). Obvious evidence for this fact is the stiffening effect during spreading of cells and the relatively high contribution to cell stiffness of certain structures such as the nucleus (THOUMINE *et al.*, 1999; CAILLE *et al.*, 2002). Furthermore, mechanical forces not only deform cells, but also induce biological responses, thereby altering their function (INGBER, 1997). For example, mechanical forces influence growth, gene expression and protein synthesis (KOMURO *et al.*, 1991; VANDENBURGH, 1992).

To understand the biomechanical effects of cell deformation, several experimental devices have been developed. These include micromanipulation techniques, micropipette aspiration, atomic force microscopes, magnetic bead manipulation techniques and cell pokers (DONG *et al.*, 1992; FRANGOS, 1993;

Correspondence should be addressed to Dr E A G Peeters; email: e.a.g.peeters@tue.nl

Paper received 25 June 2002 and in final form 11 March 2003

MBEC online number: 20033793

HAGA *et al.*, 2000; MOORE, 1994; PETERSEN *et al.*, 1982; SATO *et al.*, 1990; WANG *et al.*, 1993; ZHANG *et al.*, 1991). These devices and techniques have increased the understanding of how mechanical forces influence cell function. Of course, the design of these devices depends on the research applications and the *in vivo* loading situation they mimic (BROWN, 2000). However, none of the devices is able to monitor the biomechanical response of cells during long-term, unconfined compression of the entire cell.

The goal of the present study was to develop a device that is suitable to monitor the biomechanical response of skeletal muscle cells to sustained cell deformation. The developed device is able to measure the mechanical properties of cells and visualise the cell's structure during compression. Special attention was paid to allowing dynamic testing by using a nanopositioning system based on piezo-electric actuators. For long-term experiments, the loading device is equipped for control of temperature and CO_2. In this paper, the device is evaluated, and results of the first compression experiments are reported.

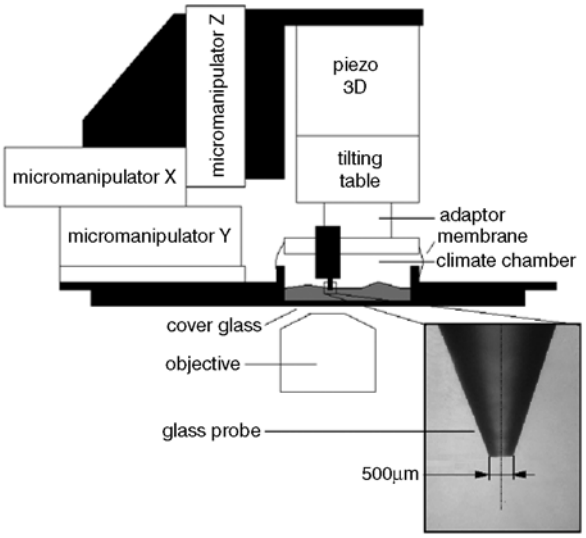

Fig. 1 *Schematic representation of loading device. Insert shows close-up of glass probe*

2 Materials and methods

2.1 *Experimental equipment*

The device for unconfined compression of individual cells is shown in Figs 1 and 2. It consists of a stainless-steel frame resting on a motorised stage of an inverted microscope* with a confocal laser scanning unit†. Normal cover glasses (25 mm in diameter) can be inserted into a polycarbonate chamber (3 mm deep and 25 mm in diameter) of the stainless-steel frame. Cells on the cover glass are compressed using a glass probe (20 mm long and 5 mm in diameter) that has a flat polished surface and a diameter of 500 µm (see insert in Fig. 1). The probe is connected to a tilting table by a polycarbonate adaptor. The tilting table can twist the adaptor plate around two axes in the horizontal plane to a maximum of 2°. This ensures that the glass probe is parallel with respect to the cover glass.

For fine positioning of the probe, the tilting table is attached to a closed-loop nanopositioning system‡, with a range of 100 µm and a resolution of 5 nm. It consists of three piezo-actuators and three strain-gauge position feedback sensors, integrated in a flexure guiding package. To displace the probe over a wider range, the nanopositioning system can be moved using three microtranslation stages** that incorporate closed-loop DC motors (range: 15 mm; minimum incremental motion: 50 nm).

Arrangements have been made to create an optimum environment for the cells, comparable with that of a CO_2 incubator. For example, a water canal surrounding the cover glass keeps the temperature of the culture medium inside the polycarbonate chamber at 37°C. The water is heated in a reservoir and pumped through the canal by a roller pump. Furthermore, a membrane spanning the gap between the chamber and the adaptor isolates the chamber from the environment. A CTI-controller†† with humidifier supplies the chamber with heated, humidified air containing 5% CO_2. For mechanical characterisation, the adaptor is replaced by a force transducer‡‡ with a full-scale range of 100 µN and a resolution of 10 nN. Specifications of the total system are summarised in Table 1.

*Axiovert 100M, Zeiss, Germany
†LSM 510, Zeiss, Germany
‡Nanocube P-611.3S, Physik Instrumente, Germany
**M-111.DG, Physik Instrumente
††Zeiss, Germany
‡‡Model 406A, Aurora Scientific Inc., Canada

2.2 *Data acquisition*

An overview of the data-acquisition system is shown in Fig. 3. The compression device is controlled by a personal computer (PC) with two 16-bit data-acquisition boards* and a motor controller PC board†. The latter, in combination with a keyboard or joystick, is used to control the position of the three microtranslation stages. The input voltage for each piezo of the nanopositioning system is supplied by a low-voltage piezo-amplifier module‡ and is controlled by the application of an analogue signal from the data-acquisition board to the input of the amplifier. A displacement sensor module** with an integrated position servo-controller compensates for hysteresis and drift of the piezos in the nanopositioning system. The actual position of the piezos can be read from the output signal of the servo-controller and is sent to the data-acquisition board. The data-acquisition board also records the output signal from the amplifier of the force transducer. A second PC controls the inverted microscope. Images of the cell are taken, if the data-acquisition card of the other PC supplies an analogue trigger signal. Custom software written in the graphical programming language LabVIEW†† controls the whole set-up and samples the signals from the force transducer and servo-controller with a sample time between 0.001 and 0.01 s.

2.3 *Experimental procedure*

In this study, the established C_2C_{12} mouse skeletal myoblast line‡‡ was used for compression experiments. Cells were seeded at low densities on cover glasses and cultured following a standard culturing protocol (MCMAHON, 1994). After one day in culture, the cells were stained with cell tracker green***, and a cover glass with cells was inserted into the polycarbonate chamber of the compression device. Fresh growth medium was added, and, after attachment of the membrane, the device was placed on the microscope stage and connected to the CTI-controller. Using the three micromanipulators, the glass probe

*PCI-6052E, National Instruments, USA
†C-842, Physik Instrumente, Germany
‡E-503.00, Physik Instrumente
**E-509, Physik Instrumente
††National Instruments, USA
‡‡ECACC, UK
***Molecular Probes, Leiden, The Netherlands

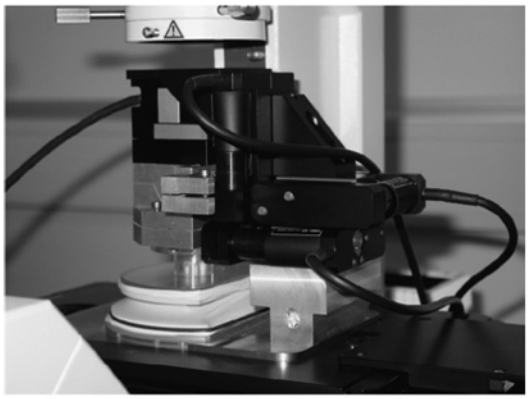

Fig. 2 *Actual realisation of loading device. Device is located on motorised stage of inverted microscope, allowing visualisation of cell during compression*

was positioned just above a single myoblast, and a three-dimensional scan was made of the undeformed cell. Then the glass probe was moved to the top of the cell by the nanopositioning system. During the actual compression experiment, the glass probe was lowered in steps of 2 μm by the nanopositioning system until the cell burst. After each step, a complete stack of confocal images was recorded so that cell deformation could be visualised.

For confocal imaging, the cells were visualised using a 20×, 0.5 numerical aperture objective*. The stain was excited by an argon ion laser with an excitation of 1% at 488 nm and a tube current of 6A. Emission was recorded above 510 nm. Three-dimensional images of the cell were taken at a sampling distance (x, y, z) of $0.22 \times 0.22 \times 0.75$ μm. The value of the eight-bit digitised signal was kept below a grey-level value of 250 to avoid electronic saturation of the photomultipliers. A full-width half-maximum (FWHM) threshold defined the boundary of the cell. With the aid of a custom software program in Matlab†, a three-dimensional rendered imaged was produced, and the width, volume and surface area of the cell were calculated before and after compression.

3 Results

3.1 *Performance*

As a skeletal muscle cell is relatively thin compared with its length, an angular twist of the probe would result in unequal compression of the cell. Non-parallelism of the probe is caused by bending of the different parts of the device, such as the micromanipulators and piezo-stage. Determination of the twist angles α and β of the probe was accomplished using the confocal microscope in reflection mode (see Fig. 4). Typical values for both angles varied between 0 and 1°, resulting in a maximum Δz of 8 μm. Before any experiment was conducted, the twist angles were returned to zero using the tilting table.

For dynamic experiments, it is important that the nanopositioning system is capable of generating an accurate sine wave and step-like signal. Therefore a pulse generator was used to generate a sine wave and a square wave, both with an amplitude of 5 μm, an offset of 5 μm and frequency of 5 Hz. Fig. 5 shows the response of the nanopositioning system as a result of the two input signals. The time delay between the input signal of the pulse generator and the output signal of the servo-controller was approximately 0.03 s. The maximum difference between the output and input signals was approximately 0.03 V, corresponding to 300 nm. Noise levels of the servo-controller corresponded to the specifications of the data-acquisition board, which has a relative accuracy of 1145 μV (~11.5 nm) at a measurable range of −10 to +10 V. This implies that noise was mainly caused by the board and not by the sensors.

*Plan Neofluar, Zeiss, Germany

†Mathworks, USA

Table 1 Specifications of single-cell loading device

maximum displacement	15 mm
minimum displacement	5 nm
maximum force	500 μN
minimum force	10 nN
compliance force transducer	10 nm μN^{-1}
frequency range	0–25 Hz
thermal stability culture chamber	±0.5°C

The design of the force transducer was based on two variable displacement capacitors, one of which was attached to the force sensing output tube of the transducer. The other one was used to compensate for thermal fluctuations and mechanical vibrations. The capacitor's plates were formed by vacuum metallisation on the surface of cantilevered fused silica beams. When a force is applied, the beam bends and the value of the capacitor changes. As long-term measurements were to be conducted using the loading device, the behaviour of two force transducers was recorded over 124 h (Fig. 6). The two transducers were located on an anti-vibration table, and no load was applied. It appeared that there was a poor correlation between the room temperature and the output of the two force transducers. Furthermore, no day cycles could be detected within the transducer's signal. Probably other effects, such as humidity and air pressure, caused this variation. Specifications regarding this drift are not provided by the manufacturer of the transducer.

To investigate whether gain or offset of the transducers changed during 24 h, the glass probe was inserted, and the force, resulting from the weight of the probe, was recorded every hour. At the start of every measurement, the amplifier output signal was set to zero by changing the amplifier offset. The mean force appeared to be 50 ± 0.05 μN, suggesting that the earlier described fluctuations were a consequence of an offset change rather than a gain change. Noise levels of the transducer were about 10 nN, which corresponded with the manufacturer's specifications.

3.2 *Deformation experiment*

Fig. 7 shows an example of a compression experiment conducted using the loading device. An individual myoblast

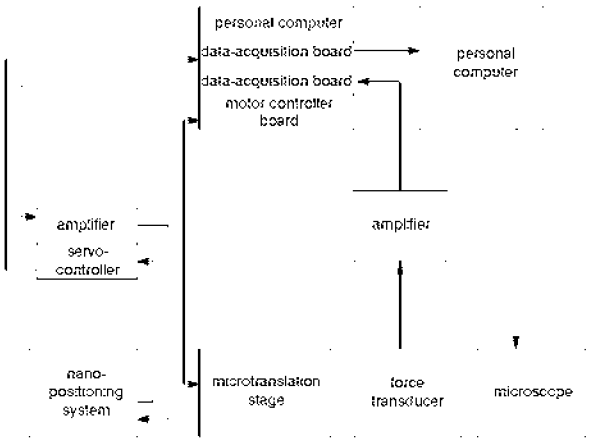

Fig. 3 *Schematic diagram of acquisition system. Total experimental set-up is controlled by two personal computers. Custom software written in Labview allows user to control set-up and record data from piezo-system, microtranslation stages and force transducer*

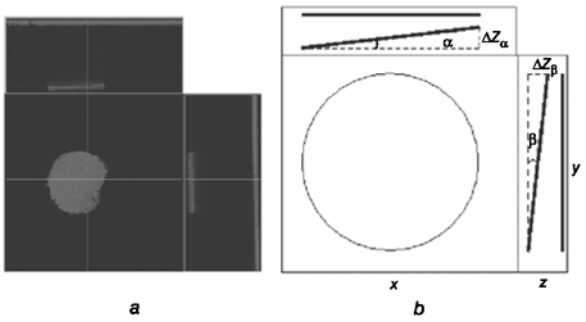

Fig. 4 *(a) Orthogonal projection of glass probe and cover glass obtained using confocal microscope in reflection mode. (b) Angles α and β can be calculated from this projection. At start of every compression experiment, these angles are reduced to zero using tilting table of loading device*

was compressed until it burst. From the orthogonal projections of the confocal images, bulges can be seen at the membrane. These bulges were probably caused by the fluorescent stain leaking out of the cell. The width of the cell was measured using the FWHM threshold (Fig. 8). From this Figure, it appears that changes in the cell's width mainly occurred during the final compression steps. The three-dimensional rendered images (Fig. 9) show the shape changes that the cell underwent as a result of compression. Volume and surface area of the cell were calculated for three steps and are presented in Table 2. The volume of the cell remained fairly constant, whereas its surface area increased. The latter was probably the result of a stretched cell membrane.

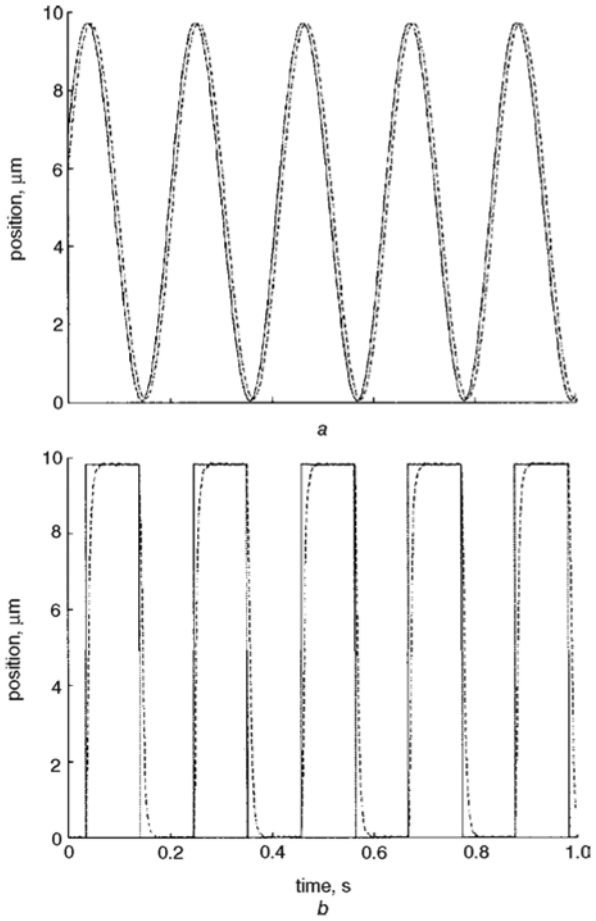

Fig. 5 *Response of nano positioning system on (a) sine wave and (b) square wave, generated with pulse generator. Both show (———) input signal for piezo-amplifier generated by pulse generator and (- - - -) output signal of servo-controller, indicating true position of nanopositioning system*

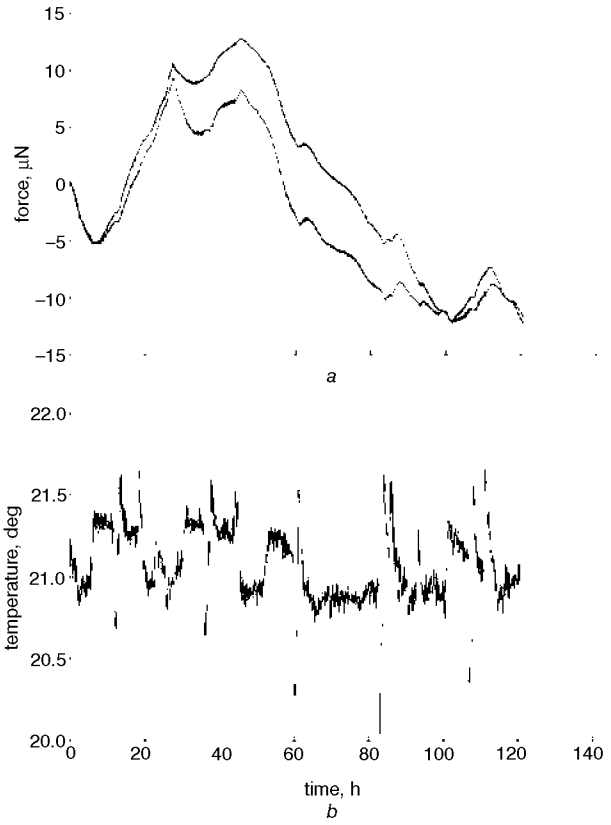

Fig. 6 *(a) Force and (b) temperature measured over period of 120 h. No loads were applied to either force transducer*

4 Discussion

The single cell loading device presented in this paper can be used to monitor the biomechanical response of skeletal muscle cells under compression. This response is reflected in changes in structure and morphology and in changes in the mechanical properties. The structure and morphology of the cell during compression was monitored using confocal laser scanning microscopy and analysed using custom image analysis software. Other micromanipulation techniques provided side views of the cell using conventional transmitted light microscopy (THOUMINE *et al.*, 1999; ZHANG *et al.*, 1991). Therefore geometric assumptions such as axisymmetry were necessary to calculate three-dimensional quantities such as volume and surface area. Unfortunately, spread myoblasts and many other cells do not have an axisymmetric shape. Thus this method provides accurate morphological measurements regardless of the geometry of the cell.

The micromanipulators allowed displacement of the probe over a wider range. Therefore multiple cells could be deformed on the same cover glass, avoiding fluctuations due to varying experimental procedures. The combination of a sensitive force transducer and a nanopositioning system created the opportunity to

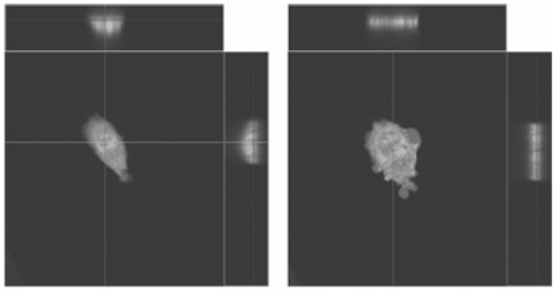

Fig. 7 *Orthogonal projections of myoblast after 0 and 10 μm axial displacement of glass probe*

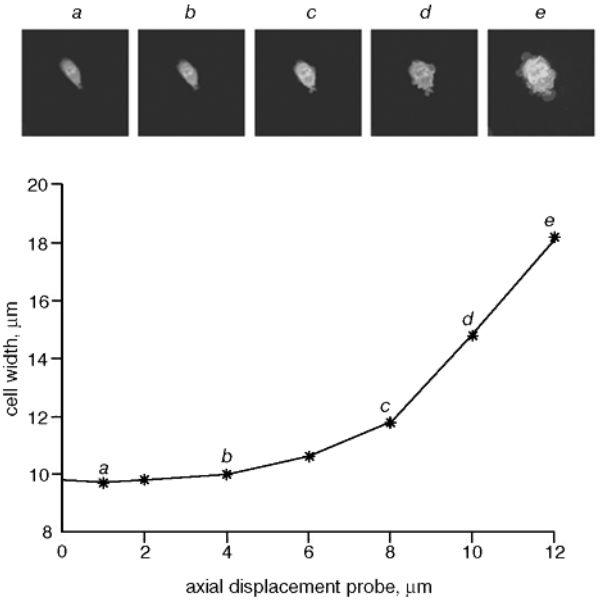

Fig. 8 *Cell width as function of axial displacement of glass probe. Cell border is defined using FWHM threshold. Horizontal confocal sections show centre of the cell at 1, 4, 8, 10 and 12 µm axial displacement of glass probe*

perform mechanical experiments. In contrast with micromanipulators, piezo-electric actuators do not experience backlash, which makes them suitable for use in dynamic experiments. Evaluation of the nanopositioning system showed good dynamic characteristics. The three strain-gauge position sensors and the position servo-controller compensate for hysteresis and drift of the piezos in the nanopositioning system.

Evaluation of the force transducer revealed its temporal instability, which was also reported in a study by BLUHM *et al.* (1995). ZHANG *et al.* (1991) showed that several micro-newtons are needed to compress animal cells, and therefore the magnitude of the measured drift can be considered to be relatively large (up to 15 µN). Despite this shortcoming, repeated weight measurements of the glass probe showed that only the offset changed in time and not the gain of the transducer. If cells are

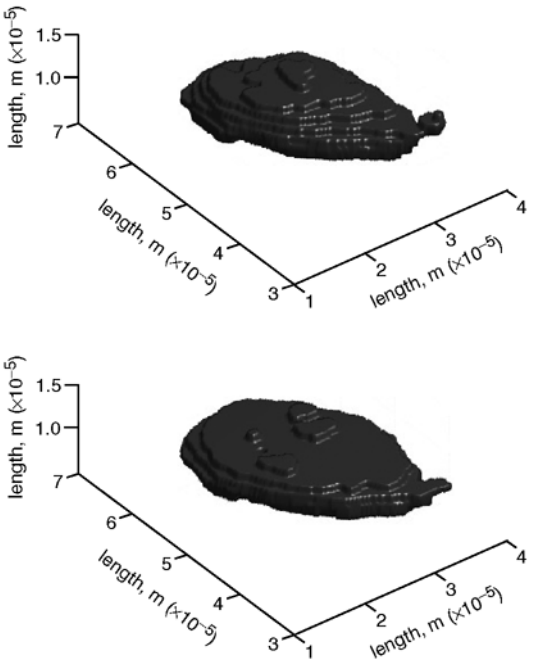

Fig. 9 *Three-dimensional rendered images of myoblast after 0 and 10 µm axial displacement of glass probe*

Table 2 Volume and surface area values of a cell, calculated from confocal images

Axial displacement probe, µm	Volume, µm^3	Surface area, µm^2
0	1050	900
6	1100	1000
10	1100	1300

mechanically characterised during long-term compression experiments, the force transducer will be set to zero, and a small load will be superimposed on the already existing load. Although absolute values of reaction forces cannot be measured, changes in the mechanical properties during long-term compression can be revealed. The position of the probe and the resulting forces during cell compression are recorded electronically and are not obtained from video images. Video images are often used in studies employing micropipette aspiration and microplates (DONG *et al.*, 1988; THOUMINE *et al.*, 1999), which may lower the temporal and spatial resolution of the method. Taken together, the use of the force transducer, the nanopositioning system and the electronic data recording allow us to perform dynamic compression tests on cells. An advantage of the device is the arrangement made to create optimum culture conditions during compression. To our knowledge, the device presented here is the first one to provide environmental conditions similar to a CO_2 incubator during compression. Similar micromanipulation techniques in other studies only heated the culture medium, because no long-term experiments have been conducted (PETERSEN *et al.*, 1982; THOUMINE *et al.*, 1999; ZHANG *et al.*, 1991). The optimised culture conditions of this experimental set-up make it possible to monitor morphological and mechanical property changes of the cell over time.

Our initial results showed total compression of an individual myoblast. The custom image analysis software provided values of several geometric cell quantities, such as width, surface area and volume. The ability to insert any tip in the loading device, with diameters up to 500 µm, makes the loading device suitable for global compression of almost every cell type and even groups of cells. Other micromanipulation techniques were designed for smaller cell types (ZHANG *et al.*, 1991; THOUMINE *et al.*, 1999) or local compression of cells (PETERSEN *et al.*, 1982; YOSHIKAWA, 1999). Furthermore, the device can be used to support other studies that examine the mechanics of cell spreading and cell attachment (RA *et al.*, 1999; THOUMINE *et al.*, 1999). The latter can be studied if the glass probe or cover glass is coated with special attachment-regulating molecules, and pulling tests are performed with the device. Another advantage of this design is the use of normal cover glasses, allowing mechanical characterisation of cells cultured on glass that is chemically treated or micropatterned (FOLCH and TONER, 2000).

Owing to the fast development of Green fluorescent protein (GFP) transfected cell lines (CUBITT *et al.*, 1995), other applications come within reach. These include, for example, real-time monitoring of a remodelling cytoskeleton or the upregulation of other proteins due to mechanical loading. On the other hand, several protein disrupting agents can be used to remove cytoskeletal filaments, so that their mechanical effects on cells can be studied with the loading device (GALBRAITH *et al.*, 1998; GUILAK, 1995). Future studies using the device are expected to reveal the visco-elastic properties of skeletal muscle cells and the deformation behaviour during compression. Furthermore, viability studies have to reveal how the magnitude and duration of deformation affect compression-induced damage or adaptation, thereby establishing thresholds for cell damage.

In summary, the device presented here provides a useful way to monitor the biomechanical response of skeletal muscle cells under

compression. The system complements other cell loading systems, owing to the use of environmental conditioning for long-term experiments, piezo-electric actuators for dynamic mechanical characterisation, and confocal imaging for observation of three-dimensional deformation. It will therefore contribute to the knowledge concerning strain-induced cell damage, as seen in pressure sores and other mechanically induced clinical conditions.

Acknowledgments—The authors would like to thank R. van den Berg and employees of the Central Technical Department for useful discussions on the design of the device and for realisation of several parts of the device. We also acknowledge the contribution of Z. Zhang (University of Birmingham, UK) to fruitful discussions on micromanipulation.

References

BARBENEL, J. C. (1991): 'Pressure management', *Prosthet. Orthot. Int.*, **15**, pp. 225–231

BLUHM, W. F., MCCULLOCH, A. D., and LEW, W. Y. W. (1995): 'Active force in rabbit ventricular myocytes', *J. Biomech.*, **9**, pp. 1119–1122

BOUTEN, C. V. C., BOSBOOM, E. M. H., and OOMENS, C. W. J. (1999): 'The aetiology of pressure sores: a tissue and cell mechanics approach', in VAN DER WOUDE, L. H. V (Ed.): 'Biomedical aspects of manual wheelchair propulsion, Assistive technology research series, vol. 5' (IOS, Amsterdam, 1999), pp. 52–62

BOUTEN, C. V. C., KNIGHT, M. M., LEE, D. A., and BADER, D. L. (2001): 'Compressive deformation and damage of muscle cell subpopulations in a model system', *Ann. Biomed. Eng.*, **29**, pp. 153–163

BROWN, T. D. (2000): 'Techniques for mechanical stimulation of cells *in vitro*: a review', *J. Biomech.*, **33**, pp. 3–14

CAILLE, N., THOUMINE, O., TARDY, Y., and MEISTER, J.-J. (2002): 'Contribution of the nucleus to the mechanical properties of endothelial cells', *J. Biomech.*, **35**, pp. 177–187

CAPLAN, A., CARLSON, B., FAULKNER, J., FISCHMAN, D., and GARETT, W. (1988): 'Skeletal muscle', in WOO, S.L.-Y., and BUCKWALTER, J. A., (Eds.): 'Injury and repair of the musculoskeletal soft tissues' (American Academy of Orthopaedic Surgeons, Park Ridge, 1988), pp. 213–291

CHEN, C. S., and INGBER, D. E. (1999): 'Tensegrity and mechanoregulation: from skeleton to cytoskeleton', *Osteoarthrit. Cartil.*, **7**, pp. 81–94

CUBITT, A. B., HEIM, R., ADAMS, S. R., BOYD, A. E., GROSS, L. A., and TSIEN, R. Y. (1995): 'Understanding, improving and using green fluorescent proteins', *Trends Biochem. Sci.*, **20**, pp. 448–455

DANIEL, R. K., PRIEST, D. L., and WHEATLEY, D. C. (1982): 'Etiologic factors in pressure sores: An experimental model', *Med. Rehabil.*, **62**, pp. 492–498

DAVIES, P. F., and TRIPATHI, S. C. (1993): 'Mechanical stress mechanisms and the cell: an endothelial paradigm', *Circ. Res.*, **72**, pp. 239–245

DONG, C., SKALAK, R., SUNG, K., SCHMID-SCHÖNBEIN, G., and CHIEN, S. (1988): 'Passive deformation analysis human leukocytes', *J. Biomech. Eng.*, **110**, pp. 27–36

ELSON, E. (1988): 'Cellular mechanics as an indicator of cytoskeletal structure and function', *Ann. Rev. Biophys. Biophys. Chem.*, **17**, 397–430

FOLCH, A., and TONER, M. (2000): 'Microengineering of cellular interactions', *Ann. Rev. Biomed. Eng.*, **2**, pp. 227–256

FRANGOS, J. (1993): 'Physical forces and the mammalian cell' (Academic Press, London, 1993)

GALBRAITH, C. G., SKALAK, R., and CHIEN, S. (1998): 'Shear stress induces spatial reorganization of the endothelial cell cytoskeleton', *Cell Motil. Cytoskeleton*, **40**, pp. 317–330

GUILAK, F. (1995): 'Compression-induced changes in the shape and volume of the chondrocyte nucleus', *J. Biomech.*, **28**, pp. 1529–1541

HAGA, H., SASAKI, S., KAWABATA, K., ITO, E., USHIKI, T., and SAMBONGI, T. (2000): 'Elasticity mapping of living fibroblasts by AFM and immunofluorescence observation of the cytoskeleton', *Ultramicr.*, **82**, pp. 253–258

INGBER, D. E. (1997): 'Tensegrity: the architectural basis of cellular mechanotransduction', *Ann. Rev. Physiol.*, **59**, pp. 575–599

KOMURO, I., KATOH, Y., KAIDA, T., SHIBAZAKI, Y., KURABAYASHI, M., HOH, E., TAKAKU, F., and YAZAKI, Y. (1991): 'Mechanical loading stimulates cell hypertrophy and specific gene expression in cultured rat cardiac myocytes', *J. Biol. Chem.*, **266**, pp. 1265–1268

KROUSKOP, T. A. (1983): 'A synthesis of the factors that contribute to pressure sore formation', *Med. Hyp.*, **11**, pp. 255–267

MCMAHON, D. K., ANDERSON, P. A. W., NASSAR, R., BUNTING, J. B., SABA, Z., OAKELEY, A. E., and MALOUF, N. N. (1994): 'C_2C_{12} cells: biophysical, biochemical, and immunocytochemical properties', *Am. J. Physiol.*, **266**, pp. C1795–1802

MOORE, S. W. (1994): 'A fiber optic system for measuring dynamic mechanical properties of embryonic tissues', *IEEE Trans. Biomed. Eng.*, **41** , pp. 45–50

NOLA, G. T., and VISTNES, L. M. (1980): 'Differential response of skin and muscle in the experimental production of pressure sores', *Plast. Reconst. Surg.*, **66**, pp. 728–733

PETERSEN, N. O., MCCONNAUGHEY, W. B., and ELSON, E. L. (1982): 'Dependence of locally measured cellular deformability on position on the cell, temperature, and cytochalasin B', *Cell Biol.*, **79**, pp. 5327–5331

RA, H. J., PICART, C., FENG, H., SWEENEY, H. L., and DISCHER, D. E. (1999): 'Muscle cell peeling from micropatterned collagen: direct probing of focal and molecular properties of matrix adhesion', *J. Cell Sci.*, **112**, pp. 1425–1436

SATO, M., THERET, D. P., WHEELER, L. T., OHSHIMA, N., and NEREM, R. M. (1990): 'Application of the micropipette technique of the measurement of cultured porcine aortic endothelial cell viscoelastic properties', *J. Biomech. Eng.*, **112**, pp. 263–268

THOUMINE, O., OTT, A., CARDOSO, O., MEISTER, J.-J. (1999*a*): 'Microplates: a new tool for manipulation and mechanical perturbation individual cells', *J. Biochem. Biophys. Methods*, **39**, pp. 47–62

THOUMINE, O., CARDOSO, O., and MEISTER, J.-J. (1999*b*): 'Changes in the mechanical properties of fibroblasts during spreading: a micromanipulation study', *Eur. Biophys. J.*, **28**, pp. 222–234

VANDENBURGH, H. (1992): 'Mechanical forces and their second messengers in stimulating cell growth *in vitro*', *Am. J. Physiol.*, **262**, R350–R355

WANG, N., BUTLER, J., and INBER, D. E. (1993): 'Mechanotransduction across the cell surface and through the cytoskeleton', *Science*, **260**, pp. 1124–1127

YOSHIKAWA, Y., YASUIKE, T., YAGI, A., and YAMADA, T. (1999): 'Transverse elasticity of myofibrils of rabbit skeletal muscle studied by atomic force microscopy', **256**, pp. 13–19

ZHANG, Z., FERNCZI, M., LUSH, A., and THOMAS, C. (1991): 'A novel micromanipulation technique for measuring the bursting strength of single mammalian cells', *Appl. Microbiol. Biotech.*, **36**, pp. 208–210

ZHU, C., BAO, G., and WANG, N. (2000): 'Cell mechanics: mechanical response, cell adhesion, and molecular deformation', *Ann. Rev. Biomed. Eng.*, **2**, pp. 189–226

Authors' biographies

EMIEL PEETERS studied Biomedical Engineering at Eindhoven University, The Netherlands. In 1999 he obtained his Master's degree on a project aimed at the mechanical characterisation of vascular prostheses. In August 1999 he started a PhD project within the research area of pressure sores prevention. The aim of the project is to examine the biomechanical response of muscle cells to deformation.

CARLIJN BOUTEN is Senior Lecturer in Tissue Engineering. In 1995 she received her PhD degree from the Eindhoven University of Technology. Her current research focusses on the mechanobiology of cells and soft tissues, applied to growth and adaptation (tissue engineered heart valves) as well as damage and deadaptation phenomena (pressure sores).

CEES OOMENS is Senior Lecturer in Biomechanics and Continuum-mechanics. He obtained his PhD at Twente University in 1985. At the present time his research is focussed on damage and adaptation of soft biological tissues. A major application field is the prevention of pressure sores.

FRANK BAAIJENS is a Professor in Soft Tissue Biomechanics & Engineering. He received his PhD degree from Eindhoven University of Technology in 1987. His interests include soft tissue biomechanics, tissue engineering, cardiovascular biomechanics and computational rheology.